HHS Public Access

Author manuscript

J Thromb Haemost. Author manuscript; available in PMC 2023 January 01.

Published in final edited form as:

J Thromb Haemost. 2022 January ; 20(1): 104–114. doi:10.1111/jth.15544.

Podoplanin promotes tumor growth, platelet aggregation, and venous thrombosis in murine models of ovarian cancer

Tomoyuki Sasano[1,*], **Ricardo Gonzalez-Delgado**[2,*], **Nina M. Muñoz**[3], **Wendolyn Carlos-Alcade**[2], **Min Soon Cho**[2], **Rahul A. Sheth**[3,&], **Anil K. Sood**[1,&], **Vahid Afshar-Kharghan**[2,&]

[1]Department of Gynecologic Oncology and Reproductive Medicine, University of Texas MD Anderson Cancer Center, Houston, Texas, USA

[2]Section of Benign Hematology, University of Texas MD Anderson Cancer Center, Houston, Texas, USA

[3]Department of Interventional Radiology, University of Texas MD Anderson Cancer Center, Houston, Texas, USA

Abstract

Background: Podoplanin (PDPN) is a sialylated membrane glycoprotein that binds to C-type lectin-like receptor 2 (CLEC-2) on platelets resulting in platelet activation. PDPN is expressed on lymphatic endothelial cells, perivascular fibroblasts/pericytes, cancer cells, cancer-associated fibroblasts, and tumor stromal cells. PDPN's expression on malignant epithelial cells plays a role in metastasis. Furthermore, the expression of PDPN in brain tumors (high-grade gliomas) was found to correlate with an increased risk of venous thrombosis.

Objective: We examined the expression of PDPN and its role in tumor progression and venous thrombosis in ovarian cancer.

Methods: We used mouse models of ovarian cancer and venous thrombosis.

Results: We showed that ovarian cancer cells express PDPN and release PDPN-rich extracellular vesicles (EVs) and that cisplatin and topotecan (chemotherapies commonly used in ovarian cancer) increase the expression of podoplanin in cancer cells. We also show that expression of PDPN in ovarian cancer cells promotes tumor growth in a murine model of ovarian cancer and that knockdown of PDPN gene expression results in smaller primary tumors. Both PDPN-expressing

[&]Correspondent author: **Contact Information**, Rahul A. Sheth, MD, T. Boone Pickens Academic Tower (FCT14.5092), 1400 Pressler St, Houston, TX 77030, Telephone: (713) 745-0652, rasheth@mdanderson.org, Anil K. Sood, M.D., Departments of Gynecologic Oncology & Reproductive Medicine and Cancer Biology, 1155 Herman Pressler, TX 77030, Houston, TX 77030, Tel 713-745-5266, asood@mdanderson.org, Vahid Afshar-Kharghan, MD, Z9.5044, Zayed Building, 6565 MD Anderson Blvd., Houston, Texas 77030, Telephone: 713-563-5267, vakharghan@mdanderson.org.

Authors' contribution

T.S.: Designed and performed experiments, analyzed and interpreted data.

R.G-D.: Designed and performed experiments, analyzed and interpreted data, and wrote the manuscript.

N.M.M.: Designed and performed experiments, analyzed and interpreted data, and wrote the manuscript.

W.C-A.: Designed and performed experiments and analyzed data.

M.S.C: Designed experiments and analyzed data.

A.K.S.: Designed experiments and analyzed data.

R.A.S.: Designed and performed experiments, analyzed and interpreted data, and wrote the manuscript.

V.A-K.: Developed concepts, designed experiments, analyzed and interpreted data, and wrote the manuscript.

[*]Contributed equally

ovarian cancer cells and their EVs cause platelet aggregation. In a mouse model of venous thrombosis, PDPN-expressing EVs released from HeyA8 ovarian cancer cells produce more frequent thrombosis than PDPN-negative EVs derived from PDPN-knockdown HeyA8 cells. Blood clots induced by PDPN-positive EVs contain more platelets than those in blood clots induced by PDPN-negative EVs.

Conclusions: In summary, our findings demonstrate that the expression of PDPN by ovarian cancer cells promotes tumor growth and venous thrombosis in mice.

Keywords

ovarian cancer; podoplanin; venous thrombosis; platelet; murine models of cancer

Introduction

Podoplanin is a membrane sialoglycoprotein with a serine/threonine-rich extracellular domain that contains four tandemly repeated platelet-aggregation stimulating (PLAG) domains and a short cytoplasmic tail [1]. Podoplanin binds to CLEC-2 on platelets and activates platelets [2–4]. Unlike PDPN that can be detected on various cell types [5], CLEC-2 is mainly expressed on platelets and megakaryocytes and to a much lesser degree on Kupffer cells in the liver [6]. PDPN is the only known ligand for CLEC-2 and activates platelets via signaling of CLEC-2 through Src /Syk/BTK/PLCγ2 [1, 7]. During embryogenesis, the interaction between PDPN and CLEC-2 has an important role in separating lymphatics from blood vessels. Deleting the gene encoding CLEC-2 in mice results in a perinatal defect in vascular development and is lethal [8–11].

Under physiologic conditions, PDPN is expressed on lymphatic endothelial cells, podocytes in kidneys, type I alveolar epithelial cells, and fibroblastic reticular cells in lymphoid organs. PDPN is not expressed on normal endothelium but can be detected in the wall of thrombosed veins [12]. Under pathologic conditions, PDPN is expressed on cancer cells, including squamous cell cancer, seminomas, osteosarcoma, and glioblastoma, on cancer-associated fibroblasts [1, 13–15]. Expression of PDPN on cancer cells mediates binding of cancer cells to platelets and promotes hematogenous metastasis in murine models [16, 17].

The interaction between PDPN and CLEC-2 plays a role in the development of venous thrombosis. Mice with CLEC-2-deficient platelets were protected against inferior vena cava (IVC) stenosis-induced thrombosis [12]. CLEC-2 deficiency reduced salmonella-induced thrombosis in hepatic vasculature [18, 19]. There is evidence that PDPN is also involved in cancer-induced thrombosis [13, 20–22]. In a study on brain tumors from patients with high-grade gliomas, increased expression of PDPN was associated with low platelet counts and an increased risk of venous thrombosis (hazard ratio for high vs. no PDPN expression: 5.71; 95% confidence interval, 1.52–21.26; P =010) [23]. In another study, injection of extracellular vesicles (EVs) from PDPN-expressing glioblastoma cells to mice resulted in platelet activation, as detected by the increase in serum concentration of platelet factor-4 (PF4) [21]. In a subcutaneous xenograft murine model of squamous cell cancer, expression of PDPN by cancer cells was associated with intra-tumor vascular thrombosis [22]. In

a recent study, mixing melanoma cells with anti-PDPN antibodies before subcutaneous injection reduced venous thrombosis induced by IVC ligation in mice [20].

This study aimed to investigate the impact of PDPN on tumor progression and venous thrombosis in a murine model of ovarian cancer. We hypothesized that PDPN expression promotes tumor growth and enhances thrombogenicity via EVs released by ovarian cancer cells.

Material and Methods

All animal studies on mice were conducted according to the Institutional Animal Care and Use Committees of the University of Texas M. D. Anderson Cancer Center.

Cell culture

The human ovarian cancer cell lines (A2780, CAOV3, HeyA8, IGROV1, OVCAR3, OVCAR4, OVCAR5, OVCAR8, OVCAR432, SKOV3, and OV8) were cultured in RPMI-1640 media, supplemented with 15% heat-inactivated fetal bovine serum (FBS), and 1% penicillin-streptomycin. The human fibroblast cancer cell line (HT1080) was cultured in Dulbecco modified Eagle medium (DMEM), supplemented with 10% FBS, and 1% penicillin-streptomycin. The human endothelial cell line (G1S1) was cultured in EBM-2 media, supplemented with 5% FBS, and growth factors (CC-4147; Lonza, Basel, Switzerland). The murine ovarian cancer cells line (ID8 and IG10) were maintained in DMEM, supplemented with 10% FBS, 1% penicillin-streptomycin, and 0.1% insulin-transferrin–sodium selenite. The murine pericyte-like cell line (10T1/2) was kept in DMEM, supplemented with 10% FBS, 1% penicillin-streptomycin, and 10 ng/mL of basic fibroblast growth factor. Cells were kept at 37°C in a humidified incubator infused with 20% O_2 and 5% CO_2.

Human ovarian cancer HeyA8 cells were incubated with cisplatin (232120; 6μM; Millipore Sigma, Burlington, MA, USA) or topotecan (T2705; 5nM; Millipore Sigma, Burlington, MA, USA) for periods of 0, 24, 48, and 72 hr; lysed and analyzed by Western blotting.

The proliferation of HeyA8 cells *in vitro* was evaluated by counting cells at regular intervals. 2.5×10^4 Hey A8-shControl or Hey A8-shPDPN were seeded per well in 6-well culture plates. The number of cells per well was quantified after 24, 48, 72, and 96 hr. For quantifying cells at each time point, cells were detached from the well and mixed with acridine orange (F23001; 1:10; Logos Biosystems, Gyeonggi-do, South Korea). The live cells concentration was measured using a LUNA-FX automated cell counter (Gyeonggi-do, South Korea).

Extracellular vesicles (EVs) isolation

We followed the “minimal information for studies of extracellular vesicles 2018 (MISEV2018) guidelines” by the International Society for Extracellular Vesicles and established sequential centrifugation methods to isolate extracellular vesicles from cancer cells [24, 25]. Cancer cells were cultured in optimal media until reaching 70–80% confluence. Then, cells were washed once with phosphate-buffered saline (PBS) and

incubated for 48 hr in media supplemented with 2% exosome-depleted FBS (Thermo Fisher Scientific, Waltham, MA, USA). The supernatant was collected and spun down 5 min at 200 g, followed by 10 min at 1,500 g to remove residual cellular debris and cells. Medium and large EVs were isolated by centrifuging supernatant for 70 min at 14,000 × g in 4°C. The pellets containing medium and large EVs were washed and resuspended in PBS. The supernatant obtained from centrifuge at 14,000 × g was centrifuged for 3 hr at 100,000 × g in 4°C to isolated small EVs. The pellets containing EVs were washed and resuspended in PBS. The protein concentration of EVs was measured using a Qubit fluorometer (Thermo Fisher Scientific, Waltham, MA, USA). EVs' size distribution was determined using the NanoSight NS300 (Malvern Panalytical, Malvern, UK). Nanoparticle tracking analysis 2.2 analytical software was used to process the data.

To investigate the impact of chemotherapy on the production of EVs by cancer cells, OVCAR8, CAOV3, and HeyA8 cells were incubated with 6μM cisplatin (232120; Millipore Sigma, Burlington, MA, USA) for 12, 24, or 48 hr in 2% exosome-depleted FBS media. The number of generated EVs was determined as described above.

Western-blotting

Protein lysates prepared from cancer cells or EVs were electrophoresed using gradient 4–20% SDS-PAGE gels and electrotransferred onto nitrocellulose membrane for immunoblotting. Membranes were blocked using 5% fat-free milk prepared in PBS containing 0.05% Tween 20 and incubated at 4°C overnight with the primary antibodies: anti-PDPN (SC-376695; 1:500; Santa Cruz Biotechnology, Dallas, TX, USA), anti-Alix (92880; 1:1,000; Cell Signaling Technology, Danvers, MA, USA), anti-Vinculin (V4139; 1:1,000; Millipore Sigma, Burlington, MA, USA), and anti-β actin (ab119716; 1:20,000; Abcam, Cambridge, UK). Membranes were incubated with horseradish peroxidase-conjugated (HRP) secondary anti-rabbit (NA9340; Cytiva, Marlborough, MA, USA) or anti-mouse (NA931; Cytiva, Marlborough, MA, USA) antibody. Bands were detected using supersignal west femto chemiluminescence HRP substrate (Thermo Fisher Scientific, Waltham, MA, USA).

Flow cytometry

Transfected HeyA8-shControl and HeyA8-shPDPN cells and their EVs were incubated with PDPN-PE antibody (337003; 1:100; Biolegend, San Diego, CA, USA) for 30 minutes at room temperature. In addition, HCS CellMask Deep Red Staining (H32721; 1:128,000; Invitrogen, Waltham, MA, USA) was used to separate the EVs from cellular debris or solution particles (EVs were PDPN-PE and CellMask double positive). An isotype-matched IgG-PE (402303; 1:400; Biolegend, San Diego, CA, USA) control antibody was used with all experimental samples. Samples were examined using the Cytek Aurora flow cytometry system (Cytek Biosciences, Fremont, CA, USA). Data were analyzed using FlowJo 10.8 software (BD Biosciences).

Generation of PDPN knockdown human ovarian cancer cell line

HeyA8 cells were transduced using lentivirus conjugated with diverse expression pGIPZ-lentiviral shRNA vectors targeting human PDPN gene: shRNA-1 (clone

ID: V2LHS_197169), shRNA-2 (clone ID: V2LHS_196451), shRNA-3(clone ID: V3LHS_401024), and shRNA-Combo (all three targeting sequences). Control HeyA8 cells were transduced with a vector containing scrambled shRNA (pGIPZ non-silencing shRNA [clone ID: RHS4346]). Transduced cells were selected using puromycin (0.6 μg/mL). shRNA vectors were purchased from the MD Anderson Cancer Center shRNA and ORFeome Core.

Platelet isolation and aggregation

Fresh blood samples were collected from healthy donors in ACD (acid-citrate-dextrose) anticoagulant, centrifuged for 10 min at 60 × g to isolate the platelet-rich plasma (PRP). Platelets were isolated from PRP using a sepharose column (2B300; Millipore Sigma, Burlington, MA, USA) with a 10-μm nylon net filter (NY1002500; Millipore Sigma, Burlington, MA, USA). Human platelets were diluted to 5×10^8 platelets/mL using PPP containing 250 μM $CaCl_2$ and 50 μM $MgCl_2$. In some experiments, PPACK (Cayman Chemical, Ann Arbor, MI, USA) at a final concentration of 80 μM was added to PRP to prevent coagulation and thrombin-induced platelet aggregation [26]. Platelet aggregation was induced by ovarian cancer cells (5×10^6 cells) or their EVs (100 ng). Platelet aggregation at 37°C with continuous stirring (1,200 rpm) was monitored in a PAP-8E optical aggregometer (Bio/Data Corporation, Horsham, PA, USA).

Murine model of ovarian cancer

Orthotopic murine model of ovarian cancer was generated by intraperitoneal injection of human ovarian cancer cells, HeyA8-shPDPN (combo) or HeyA8-shControl cells, into athymic nude mice (*Nu/Nu*, 002019; The Jackson Laboratory, Bar Harbor, ME, USA). Two million cancer cells were resuspended in 200 μl of Hank's balanced salt solution and injected into 6–8 week-old female *Nu/Nu* mice. Six weeks after the injection of cancer cells, mice became moribund and were sacrificed. Tumor nodules were resected, weighed, and fixed in formalin.

RNA isolation and RT-qPCR

RNA was extracted from the resected murine ovarian tumor nodules using RNeasy Mini Kit (74104; Qiagen, Hilden, Germany) and reverse-transcribed with verso cDNA synthesis kit (AB1453; Thermo Fisher Scientific, Waltham, MA, USA). Human and murine PDPN mRNA were quantified by amplifying cDNA using amfiSure qGreen Q-PCR Master Mix (Q5602; GenDepot, Barker, TX, USA) and the following specific primers: mouse 18s (forward 5'-GCAATTATTCCCCATGAACG-3'; reverse 5'-GGCCTCACTAAACCATCCAA-3'), human 18s (forward 5'-GAGGTAGTGACGAAAAATAACAAT-3'; reverse 5'-TTGCCCTCCAATGGATCCT-3'), mouse PDPN (forward 5'-CACCTCAGCAACCTCAGAC-3'; reverse 5'-AAGACGCCAACTATGATTCCAA-3'), and human PDPN (forward 5'-CGAAGATGATGTGGTGACTC-3'; reverse 5'-CGATGCGAATGCCTGTTAC-3'). Amplification and data acquisition was carried out using the CFX Connect Real-Time PCR Detection System and software (Bio-Rad, Hercules, CA, USA)

Immunostaining

Formalin-fixed paraffin-embedded samples were sectioned at 4 μm thickness. Slides were deparaffinized with xylene and decreasing concentrations of ethanol and rehydrated with PBS. Diva decloaker (pH 6; Biocare Medical, Pacheco, CA, USA) was used as a heat-induced antigen retriever. For immunohistochemistry, endogenous peroxidases were blocked with 3% hydrogen peroxide, and nonspecific binding was blocked using 5% horse serum. Anti-PDPN (SC-376695; 1:500; Santa Cruz Biotechnology, Dallas, TX, USA) or Ki-67 (ab15580; 1:500; Abcam, Cambridge, UK) primary antibody was diluted in blocking serum and added for overnight incubation at 4°C in a humidified chamber. A secondary biotinylated antibody was added, and the signal was amplified using a streptavidin horseradish peroxidase label kit (PK-4002 or PK-4100; Vector Laboratories, Burlingame, CA, USA). Slides were then incubated with DAB (SK-4100; Vector Laboratories, Burlingame, CA, USA) and counterstained with hematoxylin. Slides were imaged using an Olympus BX60 upright microscope. The Ki-67 labeling index of a tumor speciemen was determined by dividing the number of Ki-67 positive cells by the total number of cells counted in that tumor specimen.

For immunofluorescence examination of blood clots, nonspecific binding was blocked using 1% bovine serum albumin in PBS. CD42b primary antibody (SC-7070; 1:100; Santa Cruz Biotechnology, Dallas, TX, USA) was diluted in blocking serum and incubated overnight at 4°C in a humidified chamber. Slides are then incubated with a Cy3 conjugated secondary donkey anti-goat IgG (705-165-147; 1:1,000; Jackson ImmunoResearch, West Grove, PA, USA) and 4’,6’-diamidino-2-phenylindole DAPI (D9542; 1:1,000; Millipore Sigma, Burlington, MA, USA). Slides were imaged using either Olympus FV1000 confocal microscope. Each clot was imaged using a 10X objective lens, and composite images were generated using Image J Stitching plugin [27]. Platelet area from clots was quantified by measuring Cy3 fluorescence signal using ImageJ software.

Murine model of IVC thrombosis

An IVC stenosis model was generated as described previously [28–30]. Briefly, after anesthesia induction with isoflurane and skin sterilization with ethanol, a ventral midline abdominal incision was made. Using blunt dissection, the infrarenal IVC was isolated from the aorta. Surgical silk size 4–0 was placed securely around the IVC just caudal to the lowest renal vein. A 27G needle was temporarily placed over the IVC while the ligature was tied to provide a small lumen and prevent complete IVC ligation. The skin and abdominal wall were then closed with running sutures. The mice were then administered the EVs (or vehicle only) via tail vein catheterization. Twenty-four hours later, digital subtraction angiography was performed to evaluate the formation of IVC thrombus. Under anesthesia, iodinated contrast (Visipaque) was injected via tail vein catheterization. Digital subtraction angiography was performed using a commercial angiography system (Artis-Q, Siemens) at a frame rate of 7.5 frames/sec during contrast injection. Thrombus length measurements were then obtained from the uncompressed, diagnostic quality images using a standard PACS software platform (IntelliSpace PACS).

Statistical analysis

All statistical analysis was performed by using GraphPad Prism 8 Software. A One-way ANOVA, Holm-Sidak test, two-tailed Student t-test, or Welch's t-test was used to determining the statistical significance of comparisons. Results are presented as the mean and its standard error of the mean (s.e.) for all statistical analyses, and statistical significance was considered for $p \leq 0.05$.

Results

PDPN is expressed by ovarian cancer cells

We detected the expression of PDPN in several human and murine ovarian cancer cell lines by Western blotting. Among human ovarian cancer cell lines examined, OVCAR4, HeyA8, and CAOV3 expressed a significant amount of PDPN protein as compared to IGROV1, SKOV3, A2780, OVCAR3, OVCAR5, OVCAR8, and OVCAR432 cell lines (Figure 1A). Similarly, murine ovarian cancer cell lines ID8 and IG10 expressed high levels of PDPN. (Figure 1B). Significantly, exposure to chemotherapy agents cisplatin and topotecan increased the expression of PDPN in HeyA8 human ovarian cancer cells *in vitro* in a time-dependent fashion (Figure 1C). However, chemotherapy reagents did not affect the number of EVs released from ovarian cancer cells (Supplementary Figure 1). In addition to cell lines, immunostaining of tumor specimens from patients with ovarian cancer (Figure 1D) and tumor nodules resected from syngeneic tumors induced by ID8 murine ovarian cancer cells in C57BL/6 mice (Figure 1E) showed the presence of PDPN. In human tumor specimens, the intensity of PDPN expression by ovarian cancer cells varied in different regions of the same tumor and between different tumor specimens. Also, the expression of PDPN by fibroblasts in tumor microenvironments varied between different tumors (Supplementary Figure 2).

PDPN expressing ovarian cancer cells and their EVs induce platelet aggregation

We examined whether PDPN on ovarian cancer cells can induce platelet aggregation. One million platelets isolated from blood using sepharose column and resuspended in platelet-poor-plasma (PPP) were co-incubated with 5×10^6 ovarian cancer cells or 100 ng EVs. The formation of platelet aggregates was monitored using an optic aggregometer. While PDPN-positive HeyA8, OVCAR4, and CAOV3 cells aggregated platelets, PDPN-negative A2780 and OVCAR3 did not induce platelet aggregation (Figures 2A and 2B). EVs extracted from PDPN-positive HeyA8, CAOV3, and OVCAR4 cells induced platelet aggregation with a shorter lag time than EVs from PDPN-negative A2780 and OVCAR3 cells (Figures 2C and 2D). To further determine the role of PDPN in cancer cell-induced platelet aggregation, we reduced the expression of PDPN in PDPN-positive HeyA8 by knocking down PDPN gene expression using PDPN shRNA. We used HeyA8 cells for additional experiments because HeyA8 cells and their EVs, despite expressing PDPN express very little to no TF and have low TF activity compared to some other ovarian cancer cell lines [31]. Combining three different PDPN-shRNA (1+2+3) was the most effective in reducing PDPN expression in HeyA8 cells (Figures 3A and 3B). HeyA8-shControl cells induce more platelet aggregation as compared to HeyA8-shPDPN cells (Figures 3C and 3D). These aggregation studies were conducted in the presence of PPACK to reduce the impact of thrombin on platelet

aggregation induced by cancer cells. There was no statistically significant difference in the lag time to the initiation of platelet aggregation induced by HeyA8-shcontrol and HeyA8-shPDPN cells or their EVs.

PDPN is also expressed on EVs generated from ovarian cancer cells (Figures 3E and 3F). We showed the presence of PDPN on EVs from HeyA8-shControl cells and its reduction on EVs from HeyA8-shPDPN by Western blotting and flow cytometry (Figures 3E and 3F). We compared the ability of EVs extracted from media of HeyA8 cells transduced with PDPN-shRNA (shPDPN) to those from PDPN-scrambled shRNA (shControl) in inducing platelet aggregation. EVs from HeyA8-shPDPN were less efficient in inducing platelet aggregation as compared to EVs from HeyA8-shControl (Figures 3G and 3H).

PDPN promotes the growth of ovarian cancer in mice and is associated with a worse prognosis in humans.

We examined the effect of PDPN expressed by ovarian cancer cells on the growth of tumors in an orthotopic murine model of ovarian cancer. We injected human ovarian cancer cells (HeyA8-PDPN-shRNA or control HeyA8 cells) into the peritoneum of *Nu*/*Nu* mice. After 6 weeks, tumor nodules were resected, weighed, and processed for RNA extraction. We first established that shRNA against human PDPN effectively reduced expression of human PDPN mRNA in the tumors, but it had no effect on the murine PDPN mRNA in non-cancer cells inside tumor nodules (Figure 4A). We also observed a reduction in PDPN protein expression in tumor nodules induced by HeyA8-shPDPN compared to those induced by HeyA8-shControl (Figure 4B). PDPN knockdown significantly reduced the size of tumor nodules induced by HeyA8-shPDPN as compared to HeyA8-shControl cells (0.6 ± 0.2 g and 1.90 ± 0.5 g, respectively) (Figure 4C) and less ascites (0.2 ± 0.1 ml and 4.9 ± 1 ml, respectively) (Figure 4D).

We examined the effect of PDPN expression on the proliferation of ovarian cancer cells *in vivo* and *in vitro*. HeyA8-shControl cells did not proliferate faster than HeyA8-shPDPN cells *in vitro*, as measured by cell count over four days (Supplementary Figure 3A), but the presence of PDPN was associated with a higher proliferation index in tumor nodules resected from tumor-bearing mice, as measured by the percentage of Ki-67 positivity (Supplementary Figure 3B).

We used the TCGA database to investigate the effect of PDPN mRNA expression in tumor specimens on the prognosis of 655 patients with ovarian cancer. Our findings demonstrate that patients with high levels of PDPN expression in their tumors had worse overall survival compared to those with a lower PDPN expression (Figure 4E)(https://www.cancer.gov/tcga) [32].

PDPN expressing extracellular vesicles promotes venous thrombosis in a murine IVC stenosis model.

We extracted EVs from the cell culture media of HeyA8-shControl and HeyA8-shPDPN according to established protocols [24, 25]. The size distribution of EVs was studied with Nanosight (Supplementary Figure 4). Expression of PDPN on EVs originated from HeyA8-shControl and HeyA8-shPDPN are shown in Figure 5A. We found that medium + large

EVs and small EVs expressed PDPN, and the inclusion of small EVs did not change the expression pattern of PDPN in EVs. We injected 2×10^9 EVs from HeyA8-shControl or HeyA8-shPDPN into the tail veins of mice with surgically-induced IVC stenosis. After 24 hours, we assessed the development of IVC thrombosis in real-time via angiography (Figure 5B). Subsequently, the mice were euthanized, and IVCs with their clots were dissected. Injection of PDPN-positive EVs resulted in IVC thrombosis in 100% of mice (13/13), while PDPN-negative EVs induced IVC thrombi in 46% of mice (7/15) (Figure 5C). Injection of the saline solution alone (negative control) resulted in IVC thrombosis in none of the mice. We extracted thrombi from the resected IVCs and examined the cellular composition of thrombi by immunofluorescence staining (Figure 5D). The surface area of the thrombus section covered by platelet was measured using Image J software and used to calculate the relative platelet-rich surface area for each thrombus (platelet rich-area/total area × 100). Venous thrombi induced by PDPN-positive EVs contained more platelet as compared to thrombi induced by PDPN-negative EVs (Figure 5E). However, this difference did not show a statistical significance with the available number of thrombi.

Discussion

The correlation between PDPN expression and the increased metastatic burden has been shown in various cancer types [13, 16]. The prometastatic effect of PDPN has been attributed to its ability to mediate the adhesion of cancer cells to platelets. PDPN activates platelets by binding to CLEC-2 on platelets. Activated platelets, in turn, protect cancer cells in circulation and facilitate the extravasation of cancer cells at the metastatic niche. In addition to an indirect effect on cancer metastasis through platelet activation, PDPN expression promotes an invasive mesenchymal phenotype in cancer cells [22, 33]. In our murine model of ovarian cancer, PDPN expression by ovarian cancer cells enhanced primary tumors' growth. Tumors induced by PDPN-positive HeyA8 cells (HeyA8-shControl) in mice reached significantly larger sizes than those induced by PDPN-knockdown HeyA8 cells (HeyA8-shPDPN). It is important to emphasize that reduction in tumor size in our tumor-bearing mice was due to a lack of PDPN on cancer cells themselves. Other cells in the tumor microenvironment were originated from the host (*Nu*/*Nu* mice) and expressed PDPN.

PDPN and CLEC-2 interaction play a role in venous thrombosis in murine models. Previous studies have demonstrated that platelet-specific or universal CLEC-2 deficiency in mice reduced IVC thrombi induced by IVC stenosis. However, it did not affect thrombosis induced by IVC ligation [34]. In addition, the use of blocking antibodies to PDPN reduced intra-tumor thrombosis in metastatic melanoma lesions in lungs [35], and blocking CLEC-2 reduced venous thrombosis induced by PDPN-expressing melanoma cells in a murine model of IVC ligation [20]. In patients with high-grade gliomas, high expression of PDPN was found to be associated with a higher risk of venous thrombosis [23]. The mechanism by which PDPN on cancer cells induces thrombosis is not known. One possible explanation is that circulating cancer cells activate platelets; however, cancer cells are not present in large numbers in patients' blood, particularly in patients with gliomas. Hence, a more plausible explanation is that EVs released from cancer cells reach the bloodstream and activate platelets. Injection of PDPN-expressing EVs in mice increased the concentration of PF4 in serum, hinting toward platelet activation [21].

We showed that some ovarian cancer cell lines express PDPN, and PDPN-positive ovarian cancer cells aggregated platelets *in vitro*. EVs released from PDPN-positive ovarian cancer cells can also aggregate platelets. In mice with surgically-induced IVC stenosis, PDPN-expressing EVs caused venous thrombosis more frequently than PDPN-negative EVs. In our experiments, we monitored the development of IVC thrombosis in mice by real-time angiography. We think this is a more accurate method for documenting thrombosis than postmortem examination of IVC in mice. We noticed that lack of blood circulation during the time lapse between sacrificing and dissecting mice might result in postmortem clot formation in IVC. Furthermore, the accuracy of ultrasound-based in vivo measurements can be diminished by variations in operator technique and acoustic shadowing by overlying bowel gas.

Several factors simultaneously (either independently or synergistically) likely contribute to cancer-induced thrombosis. In our experiments, even PDPN-negative EVs induced venous thrombosis, possibly because of the presence of other thrombogenic factors (such as phosphatidylserine or tissue factor). However, PDPN-positive EVs were more efficient in causing IVC thrombosis. We have shown that tissue factor on ovarian cancer cells and their EVs contribute to venous thrombosis [31]. In a recent study, a heterogeneous expression of tissue factor and PDPN on glioblastoma cells within the same tumor was detected [21]. Injection of tissue factor expressing EVs into mice resulted in activation of the coagulation cascade, as shown by elevation in D-dimer; and injection of PDPN-expressing EVs resulted in platelet activation, as demonstrated by an increase in PF4 concentration. PDPN is not the only or even the main cause for platelet activation by ovarian cancer cells. Tissue Factor (TF) expressed by ovarian cancer cells and their EVs have an important role in platelet activation and venous thrombosis [31]. In the current study, our goal was to investigate whether PDPN on ovarian cancer cells also participates in platelet activation and venous thrombosis. We speculate that TF and PDPN have a synergistic effect on inducing venous thrombosis in ovarian cancer (and perhaps other cancers).

In our study, PDPN-expressing EVs resulted in thrombi with more platelets as compared to thrombi induced by PDPN-negative EVs. We speculate that thrombi composition may provide a clue about the dominant thrombogenic factor. For example, a fibrin-rich clot may point to a tissue factor-dependent mechanism, and a platelet-rich clot may point to a platelet-activating factor, such as PDPN, as the main culprit.

Our study on a murine model of ovarian cancer may have important clinical implications. Venous thrombosis is a significant complication of ovarian cancer. Different studies reported an incidence of VTE in ovarian cancer anywhere between 5–20%. The discrepancy in the results regarding the prevalence of VTE in ovarian cancer might be due to the more frequent use of prophylactic anticoagulation in the postoperative period [36–38]. While median survival for patients without VTE is about three years, it is reduced to 2 years in patients with VTE [39]. Because the molecular pathogenesis of cancer-associated VTE is poorly understood, available predictive models do not utilize cancer-specific risk factors. Consequently, current scoring systems are not universally accepted and have not provided sufficient evidence to establish a standard of care for outpatient thromboprophylaxis of cancer patients [40]. Although patients with more advanced stages of disease had more VTE

[41], the effect of VTE on survival is more pronounced if it occurred earlier during disease [39, 42], in the preoperative period [43], and patients with localized cancer [41]; pointing to tumor-specific risk factors that both promote VTE and an aggressive course of disease [39].

Chemotherapy increases the risk of VTE in patients with ovarian cancer [44, 45] [46]. With the more widespread use of neoadjuvant chemotherapy (NACT), the interval between ovarian cancer and surgery diagnosis has emerged as a particularly high-risk period for VTE [40]. In this study, we showed that chemotherapy agents such as cisplatin and topotecan increased the expression of PDPN on ovarian cancer cells *in vitro*. Our results raise the possibility that PDPN may link chemotherapy to an increased VTE risk in ovarian cancer.

Currently, advanced age, medical comorbidities (e.g., diabetes mellitus and obesity) [41, 47], tumor histology [43, 48, 49], cancer stage (higher stages have a higher risk) [41, 49], elevated plasma CA125 and D-dimer levels [50], anemia, thrombocytosis, and leukocytosis [51, 52] have been reported as predictive risk factors for cancer-associated VTE. Whether the addition of predictive biomarkers such as expression level of PDPN and tissue factor in ovarian cancer tumor or their concentrations in serum can enhance the predictive value of VTE scoring system needs to be studied further in additional studies on patients.

Supplementary Material

Refer to Web version on PubMed Central for supplementary material.

Acknowledgments

This work was supported by the National Institutes of Health/National Cancer Institute grants CA231141 and CA177909 to V. A-K. The authors gratefully acknowledge the assistance of Katherine Dixon, Malea Williams, and Crystal Dupuis for the in vivo IVC stenosis model generation and angiography experiments.

Disclosure of Potential Conflict of Interest:

A.K. Sood reports consulting for Astra Zeneca, Merck, and Kiyatec; receiving a research grant from M Trap; being a shareholder in Bio Path. The other authors disclose no potential conflicts of interest.

References

1. Suzuki-Inoue K, Osada M, Ozaki Y. Physiologic and pathophysiologic roles of interaction between C-type lectin-like receptor 2 and podoplanin: partners from in utero to adulthood. Journal of thrombosis and haemostasis : JTH. 2017; 15: 219–29. 10.1111/jth.13590. [PubMed: 27960039]
2. Suzuki-Inoue K, Kato Y, Inoue O, Kaneko MK, Mishima K, Yatomi Y, Yamazaki Y, Narimatsu H, Ozaki Y. Involvement of the snake toxin receptor CLEC-2, in podoplanin-mediated platelet activation, by cancer cells. J Biol Chem. 2007; 282: 25993–6001. 10.1074/jbc.M702327200. [PubMed: 17616532]
3. May F, Hagedorn I, Pleines I, Bender M, Vögtle T, Eble J, Elvers M, Nieswandt B. CLEC-2 is an essential platelet-activating receptor in hemostasis and thrombosis. Blood. 2009; 114: 3464–72. 10.1182/blood-2009-05-222273. [PubMed: 19641185]
4. Watson SP, Herbert JM, Pollitt AY. GPVI and CLEC-2 in hemostasis and vascular integrity. Journal of thrombosis and haemostasis : JTH. 2010; 8: 1456–67. 10.1111/j.1538-7836.2010.03875.x. [PubMed: 20345705]
5. Astarita J, Acton S, Turley S. Podoplanin: emerging functions in development, the immune system, and cancer. Frontiers in immunology. 2012; 3. 10.3389/fimmu.2012.00283.

6. Suzuki-Inoue K, Inoue O, Ozaki Y. Novel platelet activation receptor CLEC-2: from discovery to prospects. Journal of thrombosis and haemostasis : JTH. 2011; 9 Suppl 1: 44–55. 10.1111/j.1538-7836.2011.04335.x. [PubMed: 21781241]
7. Rayes J, Watson SP, Nieswandt B. Functional significance of the platelet immune receptors GPVI and CLEC-2. The Journal of clinical investigation. 2019; 129: 12–23. 10.1172/jci122955. [PubMed: 30601137]
8. Suzuki-Inoue K, Inoue O, Ding G, Nishimura S, Hokamura K, Eto K, Kashiwagi H, Tomiyama Y, Yatomi Y, Umemura K, Shin Y, Hirashima M, Ozaki Y. Essential in vivo roles of the C-type lectin receptor CLEC-2: embryonic/neonatal lethality of CLEC-2-deficient mice by blood/lymphatic misconnections and impaired thrombus formation of CLEC-2-deficient platelets. J Biol Chem. 2010; 285: 24494–507. 10.1074/jbc.M110.130575. [PubMed: 20525685]
9. Finney BA, Schweighoffer E, Navarro-Núñez L, Bénézech C, Barone F, Hughes CE, Langan SA, Lowe KL, Pollitt AY, Mourao-Sa D, Sheardown S, Nash GB, Smithers N, Reis e Sousa C, Tybulewicz VL, Watson SP. CLEC-2 and Syk in the megakaryocytic/platelet lineage are essential for development. Blood. 2012; 119: 1747–56. 10.1182/blood-2011-09-380709. [PubMed: 22186994]
10. Lowe KL, Finney BA, Deppermann C, Hägerling R, Gazit SL, Frampton J, Buckley C, Camerer E, Nieswandt B, Kiefer F, Watson SP. Podoplanin and CLEC-2 drive cerebrovascular patterning and integrity during development. Blood. 2015; 125: 3769–77. 10.1182/blood-2014-09-603803. [PubMed: 25908104]
11. Hess PR, Rawnsley DR, Jakus Z, Yang Y, Sweet DT, Fu J, Herzog B, Lu M, Nieswandt B, Oliver G, Makinen T, Xia L, Kahn ML. Platelets mediate lymphovenous hemostasis to maintain blood-lymphatic separation throughout life. The Journal of clinical investigation. 2014; 124: 273–84. 10.1172/jci70422. [PubMed: 24292710]
12. Payne H, Ponomaryov T, Watson SP, Brill A. Mice with a deficiency in CLEC-2 are protected against deep vein thrombosis. Blood. 2017; 129: 2013–20. 10.1182/blood-2016-09-742999. [PubMed: 28104688]
13. Suzuki-Inoue K. Platelets and cancer-associated thrombosis: focusing on the platelet activation receptor CLEC-2 and podoplanin. Blood. 2019; 134: 1912–8. 10.1182/blood.2019001388. [PubMed: 31778548]
14. Takemoto A, Miyata K, Fujita N. Platelet-activating factor podoplanin: from discovery to drug development. Cancer metastasis reviews. 2017; 36: 225–34. 10.1007/s10555-017-9672-2. [PubMed: 28674748]
15. Ugorski M, Dziegiel P, Suchanski J. Podoplanin - a small glycoprotein with many faces. American journal of cancer research. 2016; 6: 370–86. [PubMed: 27186410]
16. Lowe KL, Navarro-Nunez L, Watson SP. Platelet CLEC-2 and podoplanin in cancer metastasis. ThrombRes. 2012; 129 Suppl 1: S30–S7.
17. Suzuki-Inoue K Essential in vivo roles of the platelet activation receptor CLEC-2 in tumour metastasis, lymphangiogenesis and thrombus formation. JBiochem. 2011; 150: 127–32. [PubMed: 21693546]
18. Hitchcock JR, Cook CN, Bobat S, Ross EA, Flores-Langarica A, Lowe KL, Khan M, Dominguez-Medina CC, Lax S, Carvalho-Gaspar M, Hubscher S, Rainger GE, Cobbold M, Buckley CD, Mitchell TJ, Mitchell A, Jones ND, Van Rooijen N, Kirchhofer D, Henderson IR, Adams DH, Watson SP, Cunningham AF. Inflammation drives thrombosis after Salmonella infection via CLEC-2 on platelets. The Journal of clinical investigation. 2015; 125: 4429–46. 10.1172/jci79070. [PubMed: 26571395]
19. Nicolson PLR, Nock SH, Hinds J, Garcia-Quintanilla L, Smith CW, Campos J, Brill A, Pike JA, Khan AO, Poulter NS, Kavanagh DM, Watson S, Watson CN, Clifford H, Huissoon AP, Pollitt AY, Eble JA, Pratt G, Watson SP, Hughes CE. Low-dose Btk inhibitors selectively block platelet activation by CLEC-2. Haematologica. 2021; 106: 208–19. 10.3324/haematol.2019.218545. [PubMed: 31949019]
20. Wang X, Liu B, Xu M, Jiang Y, Zhou J, Yang J, Gu H, Ruan C, Wu J, Zhao Y. Blocking podoplanin inhibits platelet activation and decreases cancer-associated venous thrombosis. Thromb Res. 2021; 200: 72–80. 10.1016/j.thromres.2021.01.008. [PubMed: 33548843]

21. Tawil N, Bassawon R, Meehan B, Nehme A, Montermini L, Gayden T, De Jay N, Spinelli C, Chennakrishnaiah S, Choi D, Adnani L, Zeinieh M, Jabado N, Kleinman CL, Witcher M, Riazalhosseini Y, Key NS, Schiff D, Grover SP, Mackman N, Couturier CP, Petrecca K, Suvà ML, Patel A, Tirosh I, Najafabadi H, Rak J. Glioblastoma cell populations with distinct oncogenic programs release podoplanin as procoagulant extracellular vesicles. Blood advances. 2021; 5: 1682–94. 10.1182/bloodadvances.2020002998. [PubMed: 33720339]

22. Lee HY, Yu NY, Lee SH, Tsai HJ, Wu CC, Cheng JC, Chen DP, Wang YR, Tseng CP. Podoplanin promotes cancer-associated thrombosis and contributes to the unfavorable overall survival in an ectopic xenograft mouse model of oral cancer. Biomedical journal. 2020; 43: 146–62. 10.1016/j.bj.2019.07.001. [PubMed: 32441651]

23. Riedl J, Preusser M, Nazari PM, Posch F, Panzer S, Marosi C, Birner P, Thaler J, Brostjan C, Lötsch D, Berger W, Hainfellner JA, Pabinger I, Ay C. Podoplanin expression in primary brain tumors induces platelet aggregation and increases risk of venous thromboembolism. Blood. 2017; 129: 1831–9. 10.1182/blood-2016-06-720714. [PubMed: 28073783]

24. Théry C, Witwer KW, Aikawa E, Alcaraz MJ, Anderson JD, Andriantsitohaina R, Antoniou A, Arab T, Archer F, Atkin-Smith GK, Ayre DC, Bach JM, Bachurski D, Baharvand H, Balaj L, Baldacchino S, Bauer NN, Baxter AA, Bebawy M, Beckham C, Bedina Zavec A, Benmoussa A, Berardi AC, Bergese P, Bielska E, Blenkiron C, Bobis-Wozowicz S, Boilard E, Boireau W, Bongiovanni A, Borràs FE, Bosch S, Boulanger CM, Breakefield X, Breglio AM, Brennan M, Brigstock DR, Brisson A, Broekman ML, Bromberg JF, Bryl-Górecka P, Buch S, Buck AH, Burger D, Busatto S, Buschmann D, Bussolati B, Buzás EI, Byrd JB, Camussi G, Carter DR, Caruso S, Chamley LW, Chang YT, Chen C, Chen S, Cheng L, Chin AR, Clayton A, Clerici SP, Cocks A, Cocucci E, Coffey RJ, Cordeiro-da-Silva A, Couch Y, Coumans FA, Coyle B, Crescitelli R, Criado MF, D'Souza-Schorey C, Das S, Datta Chaudhuri A, de Candia P, De Santana EF, De Wever O, Del Portillo HA, Demaret T, Deville S, Devitt A, Dhondt B, Di Vizio D, Dieterich LC, Dolo V, Dominguez Rubio AP, Dominici M, Dourado MR, Driedonks TA, Duarte FV, Duncan HM, Eichenberger RM, Ekström K, El Andaloussi S, Elie-Caille C, Erdbrügger U, Falcón-Pérez JM, Fatima F, Fish JE, Flores-Bellver M, Försönits A, Frelet-Barrand A, Fricke F, Fuhrmann G, Gabrielsson S, Gámez-Valero A, Gardiner C, Gärtner K, Gaudin R, Gho YS, Giebel B, Gilbert C, Gimona M, Giusti I, Goberdhan DC, Görgens A, Gorski SM, Greening DW, Gross JC, Gualerzi A, Gupta GN, Gustafson D, Handberg A, Haraszti RA, Harrison P, Hegyesi H, Hendrix A, Hill AF, Hochberg FH, Hoffmann KF, Holder B, Holthofer H, Hosseinkhani B, Hu G, Huang Y, Huber V, Hunt S, Ibrahim AG, Ikezu T, Inal JM, Isin M, Ivanova A, Jackson HK, Jacobsen S, Jay SM, Jayachandran M, Jenster G, Jiang L, Johnson SM, Jones JC, Jong A, Jovanovic-Talisman T, Jung S, Kalluri R, Kano SI, Kaur S, Kawamura Y, Keller ET, Khamari D, Khomyakova E, Khvorova A, Kierulf P, Kim KP, Kislinger T, Klingeborn M, Klinke DJ 2nd, Kornek M, Kosanović MM, Kovács Á F, Krämer-Albers EM, Krasemann S, Krause M, Kurochkin IV, Kusuma GD, Kuypers S, Laitinen S, Langevin SM, Languino LR, Lannigan J, Lässer C, Laurent LC, Lavieu G, Lázaro-Ibáñez E, Le Lay S, Lee MS, Lee YXF, Lemos DS, Lenassi M, Leszczynska A, Li IT, Liao K, Libregts SF, Ligeti E, Lim R, Lim SK, Linē A, Linnemannstöns K, Llorente A, Lombard CA, Lorenowicz MJ, Lörincz Á M, Lötvall J, Lovett J, Lowry MC, Loyer X, Lu Q, Lukomska B, Lunavat TR, Maas SL, Malhi H, Marcilla A, Mariani J, Mariscal J, Martens-Uzunova ES, Martin-Jaular L, Martinez MC, Martins VR, Mathieu M, Mathivanan S, Maugeri M, McGinnis LK, McVey MJ, Meckes DG Jr., Meehan KL, Mertens I, Minciacchi VR, Möller A, Møller Jørgensen M, Morales-Kastresana A, Morhayim J, Mullier F, Muraca M, Musante L, Mussack V, Muth DC, Myburgh KH, Najrana T, Nawaz M, Nazarenko I, Nejsum P, Neri C, Neri T, Nieuwland R, Nimrichter L, Nolan JP, Nolte-'t Hoen EN, Noren Hooten N, O'Driscoll L, O'Grady T, O'Loghlen A, Ochiya T, Olivier M, Ortiz A, Ortiz LA, Osteikoetxea X, Østergaard O, Ostrowski M, Park J, Pegtel DM, Peinado H, Perut F, Pfaffl MW, Phinney DG, Pieters BC, Pink RC, Pisetsky DS, Pogge von Strandmann E, Polakovicova I, Poon IK, Powell BH, Prada I, Pulliam L, Quesenberry P, Radeghieri A, Raffai RL, Raimondo S, Rak J, Ramirez MI, Raposo G, Rayyan MS, Regev-Rudzki N, Ricklefs FL, Robbins PD, Roberts DD, Rodrigues SC, Rohde E, Rome S, Rouschop KM, Rughetti A, Russell AE, Saá P, Sahoo S, Salas-Huenuleo E, Sánchez C, Saugstad JA, Saul MJ, Schiffelers RM, Schneider R, Schøyen TH, Scott A, Shahaj E, Sharma S, Shatnyeva O, Shekari F, Shelke GV, Shetty AK, Shiba K, Siljander PR, Silva AM, Skowronek A, Snyder OL 2nd, Soares RP, Sódar BW, Soekmadji C, Sotillo J, Stahl PD, Stoorvogel W, Stott SL, Strasser EF, Swift S, Tahara H, Tewari M, Timms K, Tiwari S, Tixeira

R, Tkach M, Toh WS, Tomasini R, Torrecilhas AC, Tosar JP, Toxavidis V, Urbanelli L, Vader P, van Balkom BW, van der Grein SG, Van Deun J, van Herwijnen MJ, Van Keuren-Jensen K, van Niel G, van Royen ME, van Wijnen AJ, Vasconcelos MH, Vechetti IJ Jr., Veit TD, Vella LJ, Velot É, Verweij FJ, Vestad B, Viñas JL, Visnovitz T, Vukman KV, Wahlgren J, Watson DC, Wauben MH, Weaver A, Webber JP, Weber V, Wehman AM, Weiss DJ, Welsh JA, Wendt S, Wheelock AM, Wiener Z, Witte L, Wolfram J, Xagorari A, Xander P, Xu J, Yan X, Yáñez-Mó M, Yin H, Yuana Y, Zappulli V, Zarubova J, Žėkas V, Zhang JY, Zhao Z, Zheng L, Zheutlin AR, Zickler AM, Zimmermann P, Zivkovic AM, Zocco D, Zuba-Surma EK. Minimal information for studies of extracellular vesicles 2018 (MISEV2018): a position statement of the International Society for Extracellular Vesicles and update of the MISEV2014 guidelines. Journal of extracellular vesicles. 2018; 7: 1535750. 10.1080/20013078.2018.1535750. [PubMed: 30637094]

25. Pospichalova V, Svoboda J, Dave Z, Kotrbova A, Kaiser K, Klemova D, Ilkovics L, Hampl A, Crha I, Jandakova E, Minar L, Weinberger V, Bryja V. Simplified protocol for flow cytometry analysis of fluorescently labeled exosomes and microvesicles using dedicated flow cytometer. Journal of extracellular vesicles. 2015; 4: 25530. 10.3402/jev.v4.25530. [PubMed: 25833224]
26. Greco NJ, Tenner TE Jr., Tandon NN, Jamieson GA. PPACK-thrombin inhibits thrombin-induced platelet aggregation and cytoplasmic acidification but does not inhibit platelet shape change. Blood. 1990; 75: 1989–90. [PubMed: 2337670]
27. Preibisch S, Saalfeld S, Tomancak P. Globally optimal stitching of tiled 3D microscopic image acquisitions. Bioinformatics (Oxford, England). 2009; 25: 1463–5. 10.1093/bioinformatics/btp184.
28. Meng H, Yalavarthi S, Kanthi Y, Mazza LF, Elfline MA, Luke CE, Pinsky DJ, Henke PK, Knight JS. In Vivo Role of Neutrophil Extracellular Traps in Antiphospholipid Antibody-Mediated Venous Thrombosis. Arthritis & rheumatology (Hoboken, NJ). 2017; 69: 655–67. 10.1002/art.39938.
29. Yadav V, Chi L, Zhao R, Tourdot BE, Yalavarthi S, Jacobs BN, Banka A, Liao H, Koonse S, Anyanwu AC, Visovatti SH, Holinstat MA, Kahlenberg JM, Knight JS, Pinsky DJ, Kanthi Y. Ectonucleotidase tri(di)phosphohydrolase-1 (ENTPD-1) disrupts inflammasome/interleukin 1β-driven venous thrombosis. The Journal of clinical investigation. 2019; 129: 2872–7. 10.1172/jci124804. [PubMed: 30990798]
30. von Brühl ML, Stark K, Steinhart A, Chandraratne S, Konrad I, Lorenz M, Khandoga A, Tirniceriu A, Coletti R, Köllnberger M, Byrne RA, Laitinen I, Walch A, Brill A, Pfeiler S, Manukyan D, Braun S, Lange P, Riegger J, Ware J, Eckart A, Haidari S, Rudelius M, Schulz C, Echtler K, Brinkmann V, Schwaiger M, Preissner KT, Wagner DD, Mackman N, Engelmann B, Massberg S. Monocytes, neutrophils, and platelets cooperate to initiate and propagate venous thrombosis in mice in vivo. The Journal of experimental medicine. 2012; 209: 819–35. 10.1084/jem.20112322. [PubMed: 22451716]
31. Sasano T, Cho MS, Rodriguez-Aguayo C, Bayraktar E, Taki M, Afshar-Kharghan V, Sood AK. Role of tissue-factor bearing extracellular vesicles released from ovarian cancer cells in platelet aggregation in vitro and venous thrombosis in mice. Thrombosis Update. 2021; 2: 100020. 10.1016/j.tru.2020.100020.
32. Gyorffy B, Lánczky A, Szállási Z. Implementing an online tool for genome-wide validation of survival-associated biomarkers in ovarian-cancer using microarray data from 1287 patients. Endocrine-related cancer. 2012; 19: 197–208. 10.1530/erc-11-0329. [PubMed: 22277193]
33. Wu Y, Liu Q, Yan X, Kato Y, Tanaka M, Inokuchi S, Yoshizawa T, Morohashi S, Kijima H. Podoplanin-mediated TGF-β-induced epithelial-mesenchymal transition and its correlation with bHLH transcription factor DEC in TE-11 cells. International journal of oncology. 2016; 48: 2310–20. 10.3892/ijo.2016.3445. [PubMed: 27035755]
34. Lowe KL, Navarro-Nunez L, Watson SP. Platelet CLEC-2 and podoplanin in cancer metastasis. Thromb Res. 2012; 129 Suppl 1: S30–7. 10.1016/s0049-3848(12)70013-0.
35. Shirai T, Inoue O, Tamura S, Tsukiji N, Sasaki T, Endo H, Satoh K, Osada M, Sato-Uchida H, Fujii H, Ozaki Y, Suzuki-Inoue K. C-type lectin-like receptor 2 promotes hematogenous tumor metastasis and prothrombotic state in tumor-bearing mice. Journal of thrombosis and haemostasis : JTH. 2017; 15: 513–25. 10.1111/jth.13604. [PubMed: 28028907]

36. Santoso JT, Evans L, Lambrecht L, Wan J. Deep venous thrombosis in gynecological oncology: incidence and clinical symptoms study. European journal of obstetrics, gynecology, and reproductive biology. 2009; 144: 173–6. 10.1016/j.ejogrb.2009.03.012.
37. Bergqvist D, Agnelli G, Cohen AT, Eldor A, Nilsson PE, Le Moigne-Amrani A, Dietrich-Neto F. Duration of prophylaxis against venous thromboembolism with enoxaparin after surgery for cancer. The New England journal of medicine. 2002; 346: 975–80. 10.1056/NEJMoa012385. [PubMed: 11919306]
38. Schmeler KM, Wilson GL, Cain K, Munsell MF, Ramirez PT, Soliman PT, Nick AM, Frumovitz M, Coleman RL, Kroll MH, Levenback CF. Venous thromboembolism (VTE) rates following the implementation of extended duration prophylaxis for patients undergoing surgery for gynecologic malignancies. Gynecologic oncology. 2013; 128: 204–8. 10.1016/j.ygyno.2012.11.027. [PubMed: 23200912]
39. Metcalf RL, Fry DJ, Swindell R, McGurk A, Clamp AR, Jayson GC, Hasan J. Thrombosis in ovarian cancer: a case control study. British journal of cancer. 2014; 110: 1118–24. 10.1038/bjc.2014.3. [PubMed: 24448364]
40. Greco PS, Bazzi AA, McLean K, Reynolds RK, Spencer RJ, Johnston CM, Liu JR, Uppal S. Incidence and Timing of Thromboembolic Events in Patients With Ovarian Cancer Undergoing Neoadjuvant Chemotherapy. Obstet Gynecol. 2017; 129: 979–85. 10.1097/aog.0000000000001980. [PubMed: 28486358]
41. Rodriguez AO, Wun T, Chew H, Zhou H, Harvey D, White RH. Venous thromboembolism in ovarian cancer. Gynecologic oncology. 2007; 105: 784–90. 10.1016/j.ygyno.2007.02.024. [PubMed: 17408726]
42. Sørensen HT, Mellemkjaer L, Olsen JH, Baron JA. Prognosis of cancers associated with venous thromboembolism. The New England journal of medicine. 2000; 343: 1846–50. 10.1056/nejm200012213432504. [PubMed: 11117976]
43. Abu Saadeh F, Norris L, O'Toole S, Gleeson N. Venous thromboembolism in ovarian cancer: incidence, risk factors and impact on survival. European journal of obstetrics, gynecology, and reproductive biology. 2013; 170: 214–8. 10.1016/j.ejogrb.2013.06.004.
44. Fotopoulou C, duBois A, Karavas AN, Trappe R, Aminossadati B, Schmalfeldt B, Pfisterer J, Sehouli J. Incidence of venous thromboembolism in patients with ovarian cancer undergoing platinum/paclitaxel-containing first-line chemotherapy: an exploratory analysis by the Arbeitsgemeinschaft Gynaekologische Onkologie Ovarian Cancer Study Group. Journal of clinical oncology : official journal of the American Society of Clinical Oncology. 2008; 26: 2683–9. 10.1200/jco.2008.16.1109. [PubMed: 18509180]
45. Pant A, Liu D, Schink J, Lurain J. Venous thromboembolism in advanced ovarian cancer patients undergoing frontline adjuvant chemotherapy. International journal of gynecological cancer : official journal of the International Gynecological Cancer Society. 2014; 24: 997–1002. 10.1097/igc.0000000000000164. [PubMed: 24905613]
46. Swier N, Versteeg HH. Reciprocal links between venous thromboembolism, coagulation factors and ovarian cancer progression. Thromb Res. 2017; 150: 8–18. 10.1016/j.thromres.2016.12.002. [PubMed: 27988375]
47. Timp JF, Braekkan SK, Versteeg HH, Cannegieter SC. Epidemiology of cancer-associated venous thrombosis. Blood. 2013; 122: 1712–23. 10.1182/blood-2013-04-460121. [PubMed: 23908465]
48. Duska LR, Garrett L, Henretta M, Ferriss JS, Lee L, Horowitz N. When 'never-events' occur despite adherence to clinical guidelines: the case of venous thromboembolism in clear cell cancer of the ovary compared with other epithelial histologic subtypes. Gynecologic oncology. 2010; 116: 374–7. 10.1016/j.ygyno.2009.10.069. [PubMed: 19922988]
49. Bakhru A Effect of ovarian tumor characteristics on venous thromboembolic risk. Journal of gynecologic oncology. 2013; 24: 52–8. 10.3802/jgo.2013.24.1.52. [PubMed: 23346314]
50. Claussen C, Rausch AV, Lezius S, Amirkhosravi A, Davila M, Francis JL, Hisada YM, Mackman N, Bokemeyer C, Schmalfeldt B, Mahner S, Langer F. Microvesicle-associated tissue factor procoagulant activity for the preoperative diagnosis of ovarian cancer. Thromb Res. 2016; 141: 39–48. 10.1016/j.thromres.2016.03.002. [PubMed: 26967531]

51. Khorana AA, Francis CW, Culakova E, Lyman GH. Risk factors for chemotherapy-associated venous thromboembolism in a prospective observational study. Cancer. 2005; 104: 2822–9. 10.1002/cncr.21496. [PubMed: 16284987]

52. Connolly GC, Khorana AA, Kuderer NM, Culakova E, Francis CW, Lyman GH. Leukocytosis, thrombosis and early mortality in cancer patients initiating chemotherapy. Thromb Res. 2010; 126: 113–8. 10.1016/j.thromres.2010.05.012. [PubMed: 20684071]

Essentials:

- Podoplanin is a membrane protein expressed on lymphatic endothelial cells under physiologic conditions but is also expressed on cancer cells, binds to CLEC-2 and activates platelets.
- We examined whether podoplanin is expressed on ovarian cancer cells and impacts tumor growth and thrombosis.
- We showed that podoplanin is expressed on ovarian cancer cells and their extracellular vesicles.
- We showed that the expression of podoplanin enhances tumor growth in a murine model of ovarian cancer and venous thrombosis in a mouse model of inferior vena cava stenosis.

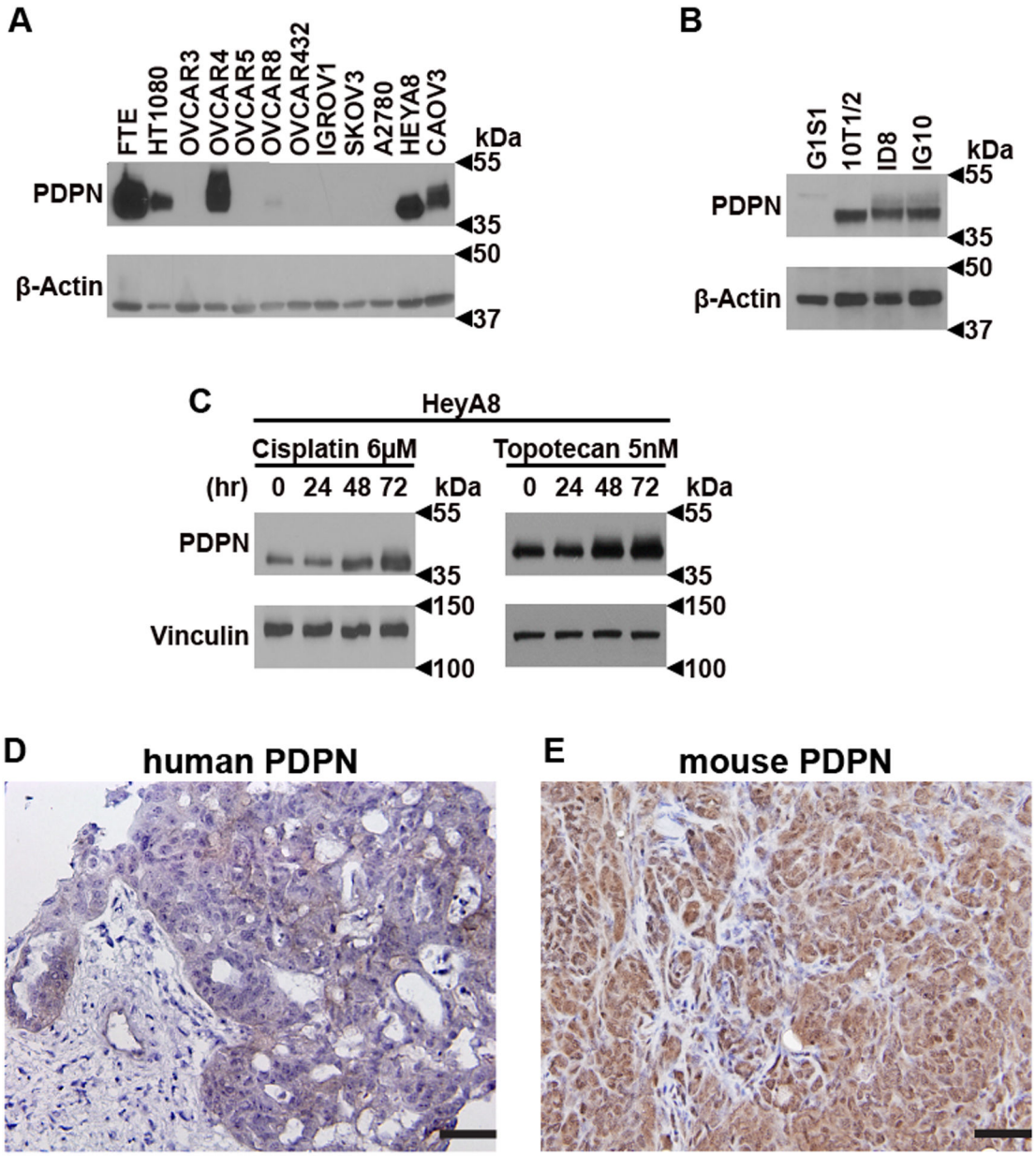

Figure 1. PDPN expression in ovarian cancer cells and tumors.

(A) Human [fallopian tube epithelium (FTE), endothelial cell line G1S1, fibrosarcoma cell line HT1080, ovarian cancer cell lines A2780, CAOV3, HeyA8, IGROV1, OVCAR3, OVCAR4, OVCAR5, OVCAR8, OVCAR432, and SKOV3] and **(B)** murine (pericyte-like cell line10T1/2, ovarian cancer cell lines ID8, and IG10) whole-cell lysates were Western blotted for PDPN. PDPN protein band is ~37 kDa, while GAPDH (~35 kDa) and β actin (~42 kDa) were used as loading controls. **(C)** PDPN expression on HeyA8 after incubation for various time intervals with cisplatin (6μM) and topotecan (5nM). Vinculin (~120 kDa) was used as a loading control. Representative immunohistochemistry (IHC) for PDPN in **(D)** human ovarian cancer tumor specimen and **(E)** a section of syngeneic tumor nodules induced by ID8 murine ovarian cancer cells in mice (Scale bar, 50 μm).

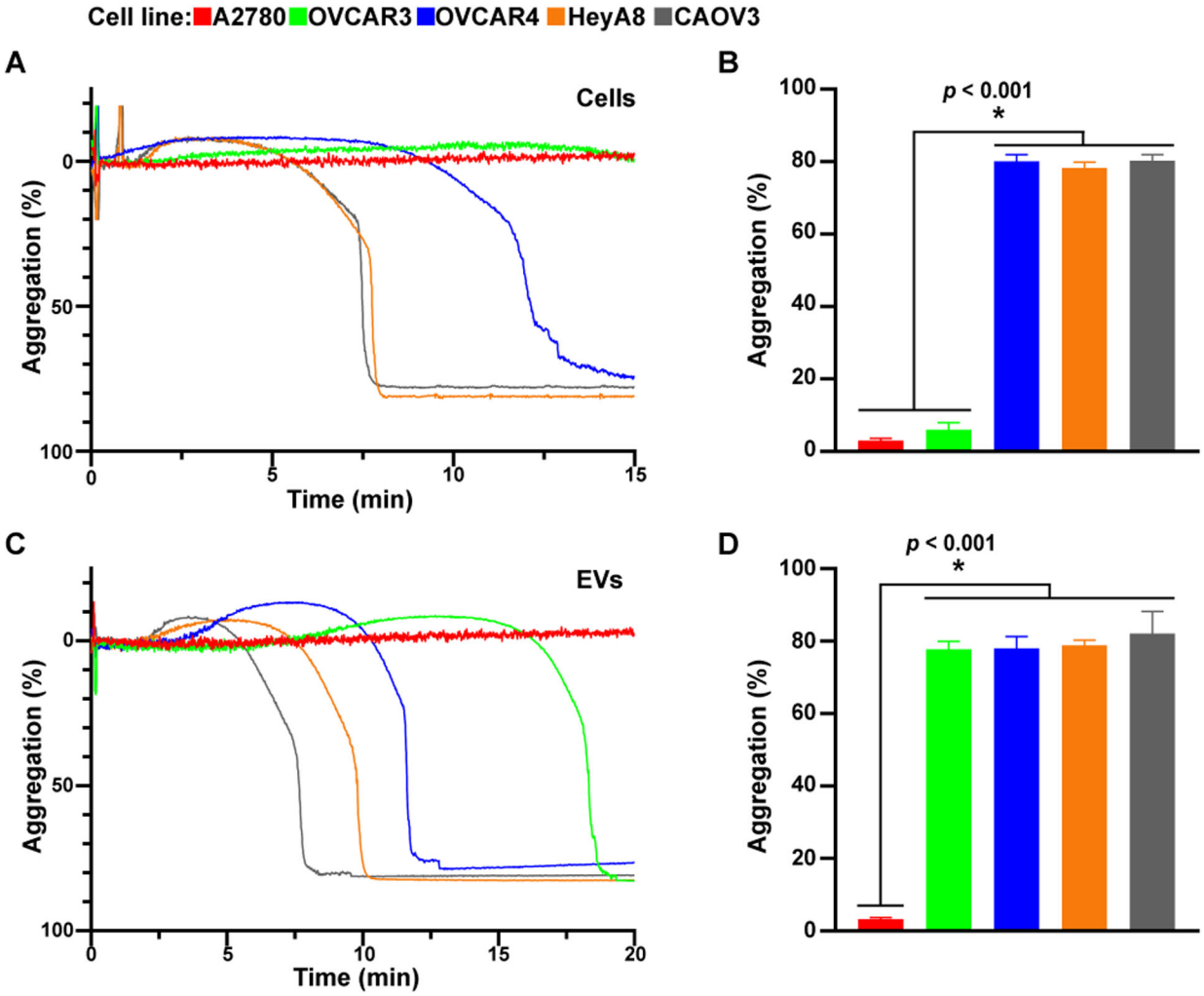

Figure 2. Effect of PDPN-positive human ovarian cancer cells and their EVs on platelet aggregation.

Representative platelet aggregation tracing induced by incubating **(A)** ovarian cancer cells (5×10^6 cells) or **(C)** their EVs (100 ng) in platelet-rich plasma (5×10^8 platelets/mL). The mean maximum platelet aggregation was compiled from several aggregation studies with **(B)** ovarian cancer cells and **(D)** their EVs ($n \geq 7$ and * = $p \leq 0.05$).

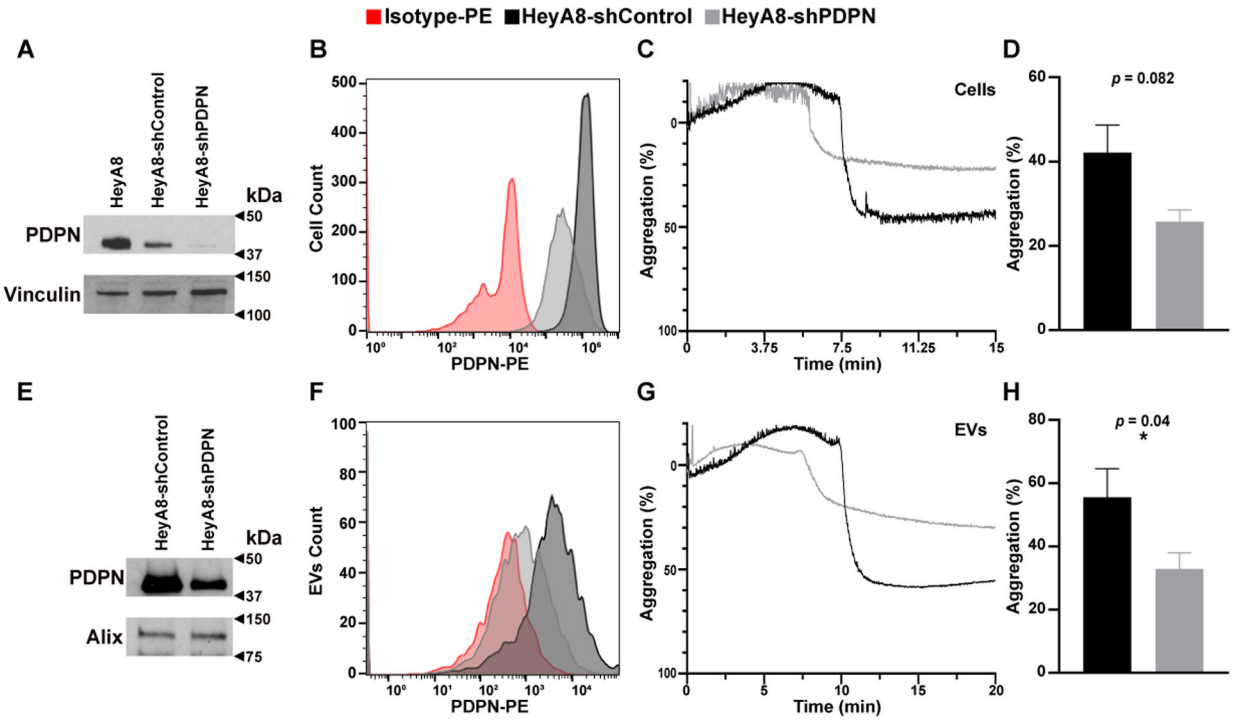

Figure 3. Effect of PDPN knockdown on platelet aggregation induced by cells and EVs.

Expression of PDPN on HeyA8, HeyA8-shControl, and HeyA8-shPDPN as detected by Western blotting of **(A)** the whole cell–lysate or **(E)** lysate from their EVs. PDPN protein band is ~37 kDa, while Vinculin (~120 kDa) and Alix (~96 kDa) were used as loading controls. PDPN expression on **(B)** HeyA8-shControl and HeyA8-shPDPN and **(F)** their EVs were detected by flow cytometry. Aggregation of human platelets induced by HeyA8-shPDPN and HeyA8-shControl cells (5×10^6 cells) or their EVs (100 ng). **(C,G)** Representative optical aggregation tracings and **(D,H)** mean maximum platelet aggregation ($n \geq 6$ and * = $p \leq 0.05$).

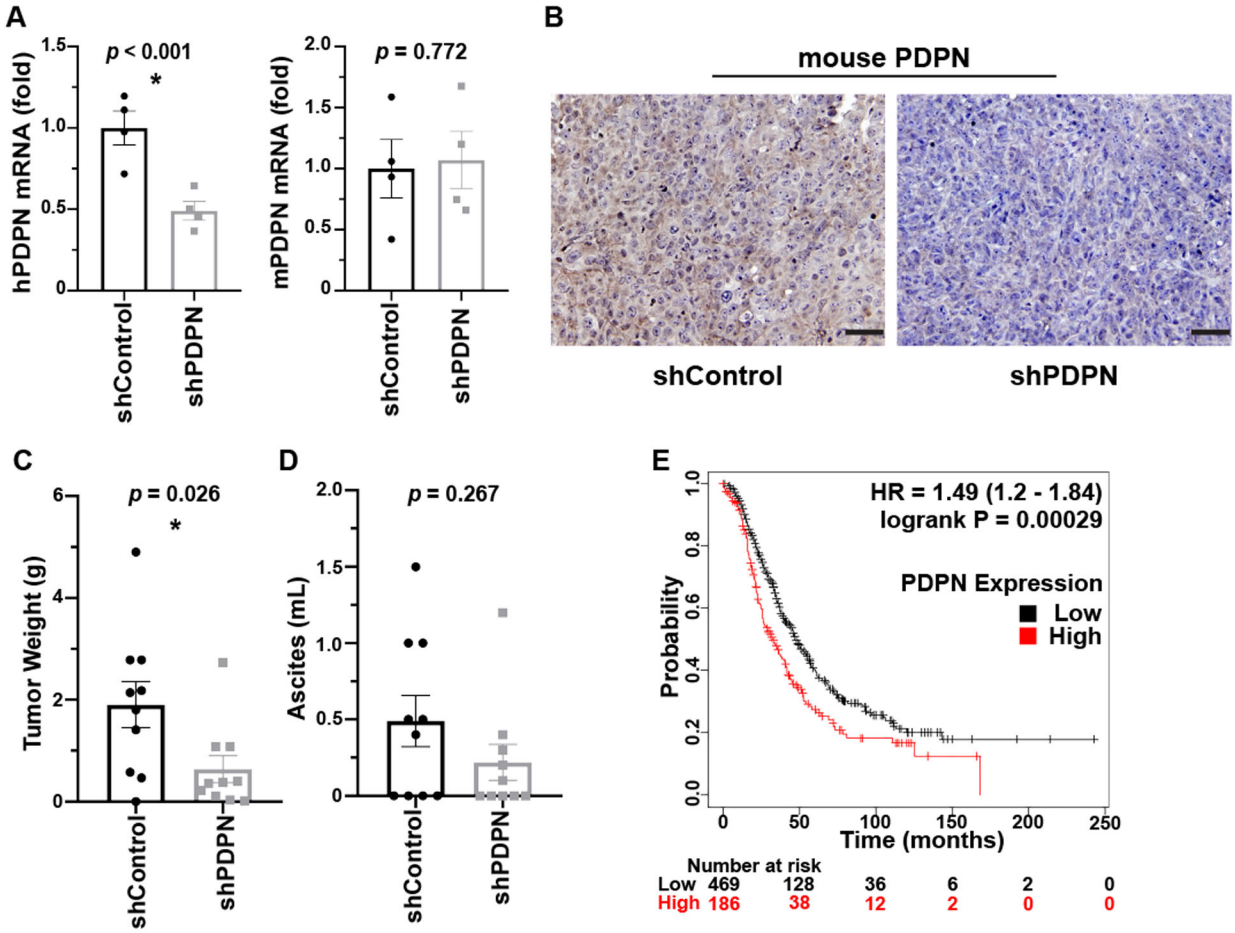

Figure 4. Role of PDPN on tumor growth in a murine model of ovarian cancer.

(A) Human and murine PDPN mRNA was quantified relative to 18s rRNA by RT-qPCR of RNA samples extracted from tumor nodules induced by human HeyA8 cells in *Nu/Nu* mice (n = 4 tumor nodules/group). **(B)** Representative IHC for PDPN in tumor nodules resected from tumor-bearing mice. Scale bar = 50 μm. **(C)** Average tumor nodules' total weight and **(D)** ascites volume was compared between mice injected with HeyA8-shControl and HeyA8-shPDPN ovarian cancer cells. n = 9–10 mice/ group. **(E)** Kaplan Meier plot comparing the overall survival in ovarian cancer patients with low (n=469) or high (n=186) PDPN expression. HR=1.49 (1.2–1.84), p = 0.00029. * = $p \leq 0.05$.

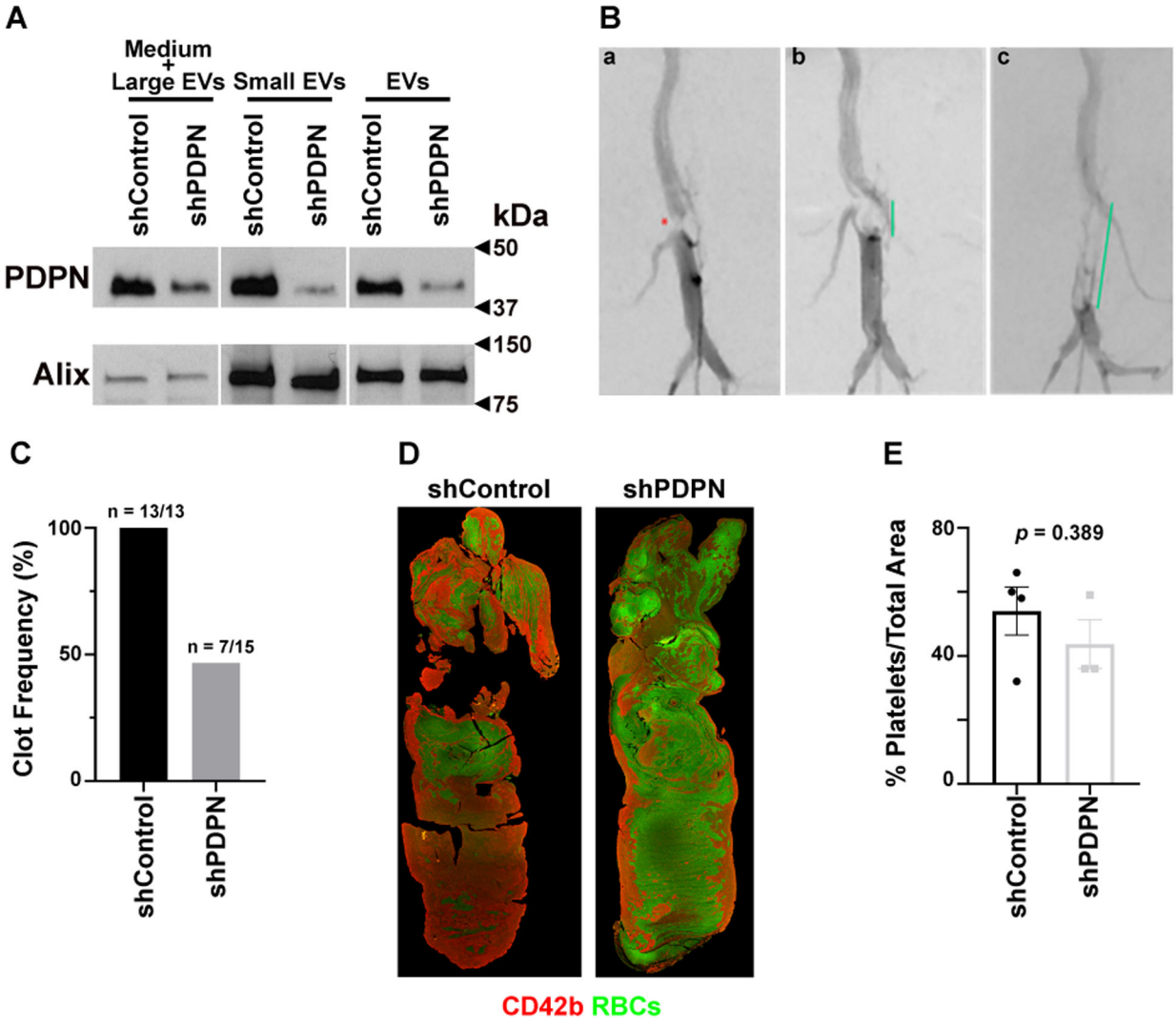

Figure 5. PDPN expression on EVs promotes venous thrombosis.

(A) Western blot analysis of PDPN expression in EVs collected from media of transduced HeyA8 cells. Cell media was centrifuged at different speeds to isolate small EVs and medium + large EVs. Alix (~96 kDa) was used as a loading control for small EVs. **(B)** Representative angiographic images of IVC stenosis and thrombosis. **(Ba)** Following IVC stenosis surgery, severe stenosis of the infrarenal IVC is notable on angiography (red asterisk). **(Bb)** Thrombus formation and **(Bc)** extension in this model recapitulates the clinical imaging findings of a filling defect within the IVC (green lines) and formation of collateral veins **(Bb, Bc)**. Red dot: IVC stenosis; green line: thrombus length. **(C)** Frequency of IVC thrombosis induced by injection of EVs from HeyA8-shControl (13 out of 13) and HeyA8-shPDPN (7 out of 15). **(D)** Representative clot structure and composition were detected by immunofluorescence microscopy after staining thrombi for platelets (red), and RBCs (green autofluorescence). **(E)** Quantification of thrombus area covered by platelets in blood clots induced by injection of EVs from HeyA8-shControl and HeyA8-shPDPN.